Accepted Manuscript

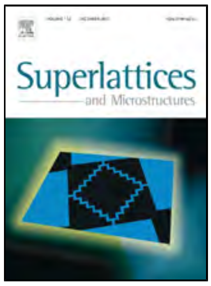

Artificial Neural Network modeling and sensitivity analysis for soiling effects on photovoltaic panels in Morocco

B. Laarabi, O. May Tzuc, D. Dahlioui, A. Bassam, M. Flota-Bañuelos, A. Barhdadi

PII: S0749-6036(17)32367-4

DOI: 10.1016/j.spmi.2017.12.037

Reference: YSPMI 5434

To appear in: *Superlattices and Microstructures*

Received Date: 30 September 2017

Revised Date: 10 December 2017

Accepted Date: 20 December 2017

Artificial Neural Network modeling and sensitivity analysis for soiling effects on photovoltaic panels in Morocco

B. Laarabi[1], O. May Tzuc[2], D. Dahlioui[1], A. Bassam[2*], M. Flota-Bañuelos[2], A. Barhdadi[1*]

[1]*Semiconductors Physics and Solar Energy Research Team (PSES)*
Energy Research Centre, Ecole Normale Supérieure (ENS)
Mohammed V University in Rabat, Morocco

[2]*Faculty of Engineering, Autonomous University of Yucatan,*
Av. Industrias no contaminantes, Merida, Yucatan, Mexico

Abstract

In the present work, an Artificial Neural Network (ANN) methodology for studying and modeling the soiling effect on solar photovoltaic (PV) glass is presented. To perform the study, a solar PV glazing was exposed outdoor at the home solar energy platform of Physic of Semi-conductors and Solar Energy research structure (PSES) at Mohammed V University in Rabat, Morocco. Regular measurements from April 20, to December 31, 2016, were carried out to monitor the soiling rate changes over time. Meteorological data were used as input variables for ANN modeling. The model performance was evaluated using a statistical comparison between experimental and simulated values. Results show that the implementation of Levenberg-Marquardt backpropagation algorithm, and the active functions Tansig, and Purline achieve the best estimations ($R^2 = 0.928$) in an ANN architecture 6-35-1. Additionally, a sensitivity analysis approach was employed to determine the effect of input parameters on model output and the behavior of the model with the variation of each input parameter. Sensitivity analysis results indicate that the most influential parameter for PV soiling rate was the relative humidity, followed by wind direction. The ANN model coupled with sensitivity analysis show be a promising framework for its application in smart sensors on cleaning systems for PV modules to improve their operational efficiency.

Keywords: Solar energy; soiling effect; solar PV glass; ANN application; PAWN sensitivity analysis.

---

*Corresponding author
Email address: abarhdadi@yahoo.fr (A. Barhdadi)
Email address: baali@correo.uady.mx (A. Bassam)

Preprint submitted to Superlattice and Microstructure *11/27/2017*

1. INTRODUCTION

Morocco is considered the largest potential markets for renewable energies in the region of Meddle East and North Africa (MENA), thanks to excellent solar resources throughout the country and wind resources along Atlantic Coast [1]. The potential of solar energy in Morocco is estimated at 3000 hours/year, hence the launch of the Moroccan Solar Plan to reach 2 Gigawatts by 2020. Unfortunately, the sites where the solar energy is important, characterized, in most cases, by harsh weather conditions which can increase the probability of material degradation and also provoke severe dust accumulation [2]. This last parameter is named soiling or dusting and it is mostly a mixture of small amounts of organic particles and/or minerals from geomorphic fallout such as sand, clay, or eroded limestone.

In Morocco, just a few studies have been conducted in order to study the effect of this phenomenon on the performances of PV (Photovoltaic)/CSP (Concentrated Solar Power) modules and systems. Table 1 presents a summary of the studies performed in Morocco, their locations as well as their results. From this, it can be clearly seen that six studies have been conducted in eight Moroccan cities belonging to semi-arid, arid, and extremely arid climates. They all proving the relevance of the topic considered in this work. The studies include the losses during the exposure period, the effect of tilt angle, the determination of factors affecting soiling, and modeling of this phenomenon using time series. It can also be seen that modeling of soiling phenomenon in Morocco still need more studies, which prove that each addition in that subject will be of such importance.

Table 1. Studies of soiling effect on PV/CSP modules conducted in Morocco

Category	Technology	Region	Results	Ref
Investigation	CSP	Skoura (40 km from Ouarzazat)	The soiling rate is a function of the variation of the wind speed and the relative humidity during the exposure.	[3]
	CSP	Oujda	The drop in cleanliness is: - 45% and 33% for glass and mirrors in aluminum, respectively in a horizontal position. - 14% for both reflectors at an angle of +45°. For mirrors installed at 0° and -45° angles remained clean with a purity average of about 97% for both types of mirrors.	[4]
	PV-modules irradiation sensors	Atlantic Ocean	The efficiencies dropped to 20% of the initial values within 5 months.	[5]
	CdTe PV	Marrakech, Ouarzazate,	Estimates of the change in average monthly CdTe PV performance due to soiling are 0 to <-3% with cleaning.	[6]

		Oujda, Dakhla		
	PV/HCPV (High Concentration Photovoltaics)	Rabat	Transmittance losses of a solar PV glass due to soiling are approximately 5% per three months. Productivity losses of HCPV modules are approximately 7,64% per one month.	[7] [8]
Modelling	CSP	Tantan, Agadir	The analysis of the cleanliness of a solar reflectors exposed outdoors has been performed using the free R software for statistical computing and graphics. The results have shown that the best-fitted model describing the long-term change in the cleanliness is the local linear trend, which performs even better when an optimal discount factor of 0.95 is considered.	[9] [2]

Soiling is depending on several parameters which have a double effect in most cases. These parameters can be gathered into five different groups: the nature of the surface, the weather conditions, the soiling properties, the exposure conditions, and the environmental conditions. Table 2 summarizes the various parameters as well as their effects on soiling. In this table we have tried to describe for each condition (higher, lower, big, small…) of each factor (wind speed, rainfall, tilt angle…) the nature of its effect, positive (+) or negative (-). We have also described the arguments behind this nature based on studies published in literature.

The content of this table shows the complexity of the soiling phenomenon because of depending on several environmental parameters at the same time. It is also proving that extensive investigations should be conducted with the objective to understand well this phenomenon.

The parameters mentioned in this table could be divided into two categories, static parameters and temporal parameters. The static parameters depend on recommendations of standards (nature of the surface, tilt angle), physical laws such as gravity (location) or the existing specifications of the chosen site (soil texture). The temporal parameters comprise weather conditions and soiling properties and they changed through time and differ from a season to another. Concerning the tracking it is a parameter that change through the day and from a season to another but it can be considered as static from a year to another. For birds dropping, it’s a complex parameter that is difficult to predict. From this we can conclude that the weather conditions and soiling properties are the most relevant parameters affecting this phenomenon. Based on this conclusion we have tried to predict the effect of soiling from some weather conditions factors. Some of them, have been chosen from Table 1 and other ones have been added in order to study their effect. The soiling properties and other parameters will be included in the future improved model.

Table 2. Summary of the different parameters that could impact the soiling of PV modules.

Nature of the effect	Parameters	Conditions	Effect	Arguments	Ref
Nature of the surface	Nature of the surface	Low surface energy. Chemically neutral, smooth and hydrophobic surface.	+	Reduction of the adhesion forces of particles to the surface.	[10] [11]
Weather conditions	Wind speed	higher	+	Removal of dust from the surface.	[12] [13]
			-	The increase of aerosols in the air.	
	Moisture	Higher	+	Increased interparticle forces of soil particles, therefore, the need for high speeds for their transport.	[10] [11]
			-	The increase of interparticle forces of the particles deposited on the surface of the module, therefore, the need for high speeds for their transport.	
	Dew		-	Promoting cementing and adhesion of particles.	[14] [15]
	Rainfall	Heavy	+	Cleaning modules.	
		Low	-	Promoting cementing and adhesion of particles.	
Soiling properties	Particle Size	Small	- (Compared to big particles)	Shading of all the module surface	[13]
		Big	+ (Compared to small particles)	Shading of part of the module surface.	
	Composition	Opaque	-	Decrease the transmitted irradiance.	[11] [12]
		Translucent	+	Increase the transmitted irradiance.	
		Transparent			
Exposure conditions	Tilt angle	Large	+	Removal of dust due to gravity.	[16]
		Low	-	Significant accumulation of dirt.	
	Location	Top	+	Less dust accumulation.	[16]
		Low	-	Large dust accumulation.	
	Tracking	With	+	Less dust accumulation.	[16]
		Without	-	Large dust accumulation.	
Environmental conditions	Bird droppings	In off-shore sites	-	Shading cells and creating hot spots.	[16]
	Soil texture	Compacted	+	Low concentration of aerosols in the air.	[12]
		Loose with sand	-	The increase of aerosols in the air.	

It is extremely difficult to study experimentally the PV panel losses due to soiling everywhere, and there is an urgent need to model this phenomenon using appropriate innovative approaches. Indeed, many countries are giving a high priority to developing accurate soiling loss modeling and forecast soiling effect over time. In the last years, Artificial Neural Networks (ANN) have been employed as a suitable tool for modeling phenomena in PV systems, due to their robustness, noise tolerance and their ability to work with multivariable and non-linear information. These techniques have been successfully applied on PV systems for various purposes such as model the performance and the daily PV energy power production [17,18]; temperature estimation for PV modules and PV arrays [19,20]; modeling of characteristic curves for the development of new PV semiconductor materials [21,22]; and implementation in Maximum Power Point Tracking (MPPT) PV systems [23], to mention a few. In all these works, ANNs have been described as a suitable tool for modeling different phenomena occurring in PV systems.

The aim of this work is to present an ANN methodology for modeling the soiling effect on solar PV glass based on meteorological parameters. Additionally, a new sensitivity analysis approach is proposed in order to determine the relative importance of the meteorological parameters on the PV glass soiling effect. The paper is organized in the following way. The next section constrains the experimental set-up description, the artificial neural network theory, and the sensitivity analysis technique explanation. The third section presents the results and discussions of ANN modeling and sensitivity analysis influence. Finally, in the last section, the conclusions are pointed out.

2. MATERIAL AND METHODS

2.1. Description of experimental design

To perform the study, a solar PV glazing (Figure 1(a)) was exposed outdoor at home Solar Energy Platform in Rabat. Regular measurements from April 20 to December 31, 2016, were performed to monitor the change of soiling rate over time.

In this work, the effect of meteorological parameters (global solar irradiance, wind velocity, wind direction, ambient temperature, relative humidity, and rainfall) on the soiling rate of solar PV glass has been studied. Meteorological data have been recorded both from the weather station (Figure 1(b)) installed in the Solar Energy Platform and from the Moroccan Meteorology Department.

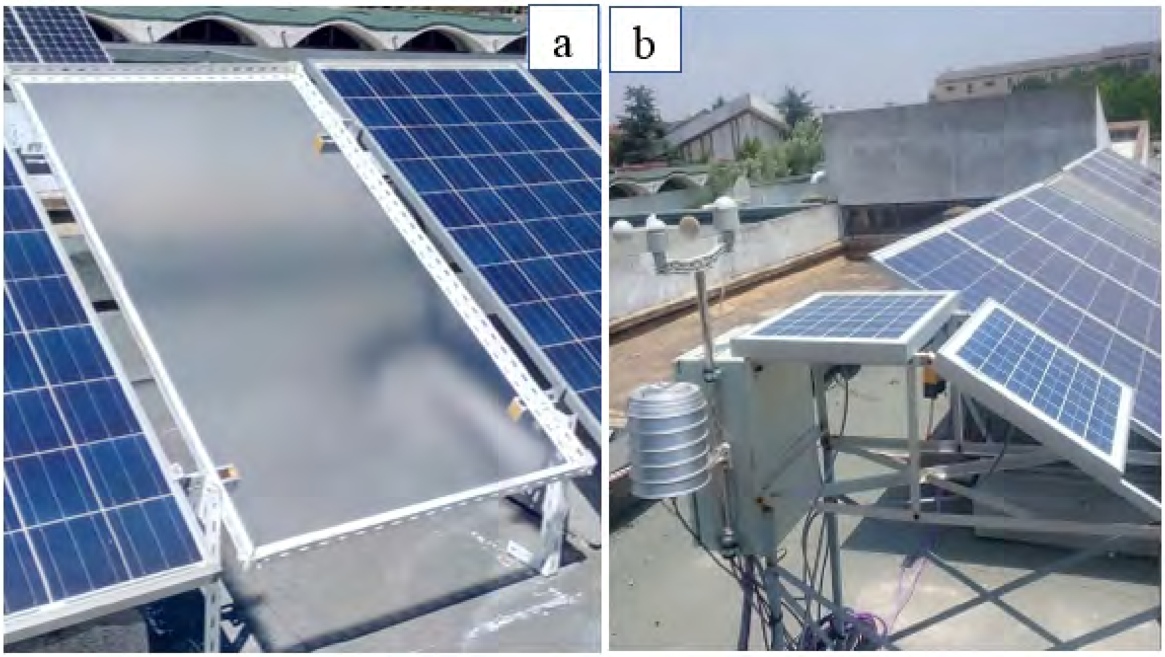

Figure 1. a) The solar PV glass installed in the outdoor conditions of Rabat-Morocco. b) The meteorological station installed in the solar energy platform of PSES, ENS-UM5-Rabat.

The soiling rate has been calculated using the following equations:

$$??_e = \frac{G - G_{moy}}{G} \tag{1}$$

$$G_{moy} = \frac{\sum_{i=1}^{i=24} G_i}{24} \tag{2}$$

G and G_{moy} are respectively the received and the transmitted irradiance by the solar PV glass. The average transmitted irradiance was calculated by performing various spot irradiance measurements. The experimental procedure is as follows:

1. The standard solar PV glass used in our experiment is supposed divided into 24 elementary rectangles of equal dimensions (27.5 cm x 24.5 cm).

2. For each elementary rectangle, the received irradiance G and the transmitted one G_i are regularly measured every day at noon, using a solar power meter placed at the center of both sides of the rectangle. This operation takes an average time of about 6 minutes.

3. The transmitted irradiance G_{moy} over the whole surface of the solar PV glass is then determined by calculating the arithmetical average of the 24 G_i measured.

G_i and G both have been measured using a solar power meter.

2.2. Artificial Neural Network approach

Artificial Neural Networks (ANN) are artificial intelligence algorithms inspired by the functioning of the nervous system. They are integrated by a number of interconnected units, called neurons, that present a natural tendency to learn from the information of the outside world. The main characteristic of these models is that they do not require knowledge of the study phenomenon [24].

ANN are used to estimate functions that depend on a large number of parameters. In an ANN neuron, each input parameter is assigned with an appropriate weighting factor (**W**). The sum of the weighted inputs and the bias (**b**) is evaluated in a transfer function which generates an output value that interacts with other neurons [25]. The architecture of ANN is usually divided into three parts: an input layer, a hidden layer(s) and an output layer (Figure 2). To solve the non-linear multivariable phenomena, ANN are subjected to an iterative process called training. This process is performed using specific algorithms, where one of the most used is the Back-Propagation [22]. In the training process, the network modifies the weights and bias values according to the computed error between simulated output and experimental samples, a process that is repeated until obtaining a model that describes accurately the studied phenomenon. The trial and error approach is the most basic method for training a neural network.

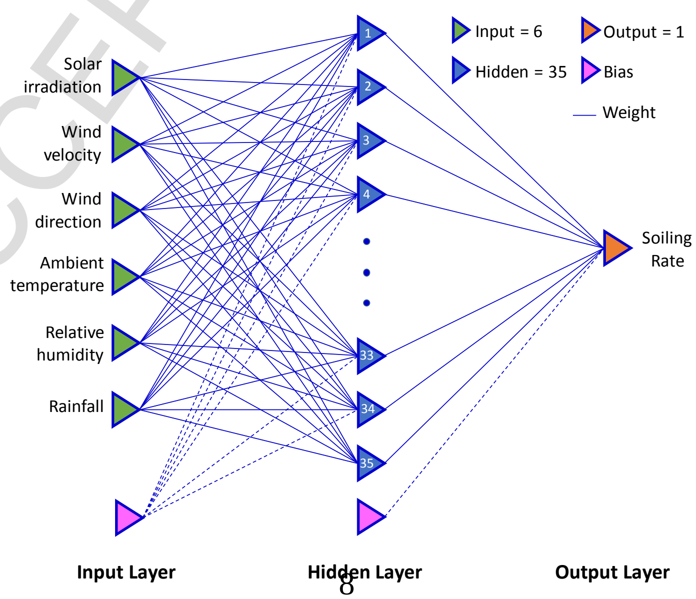

Figure 2. Artificial Neural Network architecture for soiling rate estimation.

2.3. Mathematical modeling development

An iterative numerical procedure was conducted in order to train and determine the ANN model that provides the best PV glass soiling rate estimation. The implemented procedure consists of three steps: (I) Creation and segmentation of the working database, (II) ANN architectures design and training, and (III) statistical comparison of ANN models. A graphical synthesis of the computational methodology is illustrated in Figure 3.

(I) A working database was formed based on the parameters recorded by the measurement equipment: solar irradiance [68 W/m^2, 1182 W/m^2], wind speed [0.13 m/s, 2.74 m/s], wind direction [0°, 350°], ambient temperature [11.4 °C, 31.2 °C], relative humidity [28%, 89%], rainfall [0 mm, 32.7 mm], and PV glass soiling rate [1.65%, 19.84%]. Table 3 synthesizes the presented data sets.

Table 3. Parameters used for the mathematical modeling process.

Parameters		Min	Max	Units
Inputs				
Solar irradiance	(G)	68	1182	[W/m^2]
Wind speed	(W_s)	0.13	2.74	[m/s]
Wind direction	(W_d)	0	350	[°]
Ambient temperature	(T_{amb})	11.4	31.2	[°C]
Relative humidity	(RH)	29	89	[%]
Rainfall	(RF)	0	32.7	[mm]
Output				
PV glasses soiling rate	(SR)	1.65	19.84	[%]

Previous to the training process, the working database was normalized between 0.1 and 0.9 to avoid numerical overflows because of very large or small weights [26]. Database normalization was given by the following equation:

$$x = \frac{X_i}{1.1 \times X_{max}} \tag{3}$$

where x represents the normalized value of X_i, and X_{max} is the maximum value of X_i. The database was randomly divided into three segments for ANN training process: 80 % was destined to training phase, 10 % for validation phase, and 10 % for testing. The random division was used to guarantee the accurate representation of the data distribution.

(II) To obtain a model that provides reliable estimations of PV glass soiling rate, several ANN architectures were evaluated. Figure 2 illustrates the basic ANN architecture used, it is composed of 6 neurons in the input layer corresponding to solar irradiance, wind speed, wind direction, ambient temperature, relative humidity, and rainfall; and one neuron in the output layer given by the PV glass soling rate. The transfer functions employed for nonlinear solutions are the hyperbolic tangent sigmoid (*Tansig*, Eq. 4) for the hidden layer and the linear transfer function (*Purline*, Eq. 5) for the output layer [27]:

$$Tansig(n) = \frac{1}{1 + exp\,(-2n)} - 1 \tag{4}$$

$$Purline(n) = n \tag{5}$$

where n represents the weighted sum of the input values. The Levenberg-Marquardt (LM) backpropagation algorithm (a derivation of the Newton method) was employed to obtain the optimum weights and bias values for the ANN models, due to being one of the most successful algorithms in increasing the convergence speed of an ANN architectures [28]. Moreover, an architecture with a single hidden layer was used, because it presents a simpler computation and fewer weights error propagation compared to architectures with two or more hidden layers [29,30]. The progressive increment of neurons in the hidden layer was the computational strategy used to find out the appropriate network architecture.

(III) To measure the estimation accuracy of the ANN architecture, statistical comparisons between simulated outputs and experimental values were conducted. The mathematical error criteria used for the comparisons were the Root Mean Square Error (RMSE) used to measure the difference between the model predicted respect to the experimental measures; the Mean Absolute Percentage Error (MAPE) that computes the percentage error of the model numerical estimates; and the Coefficient of Determination (R^2) determines the linear relationship between experimental and simulated data between (0, 1) [31]:

$$RMSE = \sqrt{\frac{\sum_{i=1}^{n}\left(SR_{Exp(i)} - SR_{Sim(i)}\right)^2}{n}} \tag{6}$$

$$MAPE = \frac{\sum_{i=1}^{n}\left|\frac{SR_{Exp(i)} - SR_{Sim(i)}}{SR_{Exp(i)}}\right|}{n} \times 100 \tag{7}$$

$$R^2 = 1 - \frac{\sum_{i=1}^{n}\left(SR_{Exp(i)} - SR_{Sim(i)}\right)^2}{\sum_{i=1}^{n}\left(SR_{Exp(i)} - \overline{SR}_{Exp}\right)^2} \tag{8}$$

where $SR_{Exp(i)}$ is the measured PV glass soiling rate, $SR_{Sim(i)}$ is the simulated ANN output, and $\overline{SR}_{Exp}$ is the average experimental PV glass soiling rate. As it can be appreciated in Figure 3, while these statistical criteria are not satisfactory, the architecture of ANN is modified and the training process is repeated.

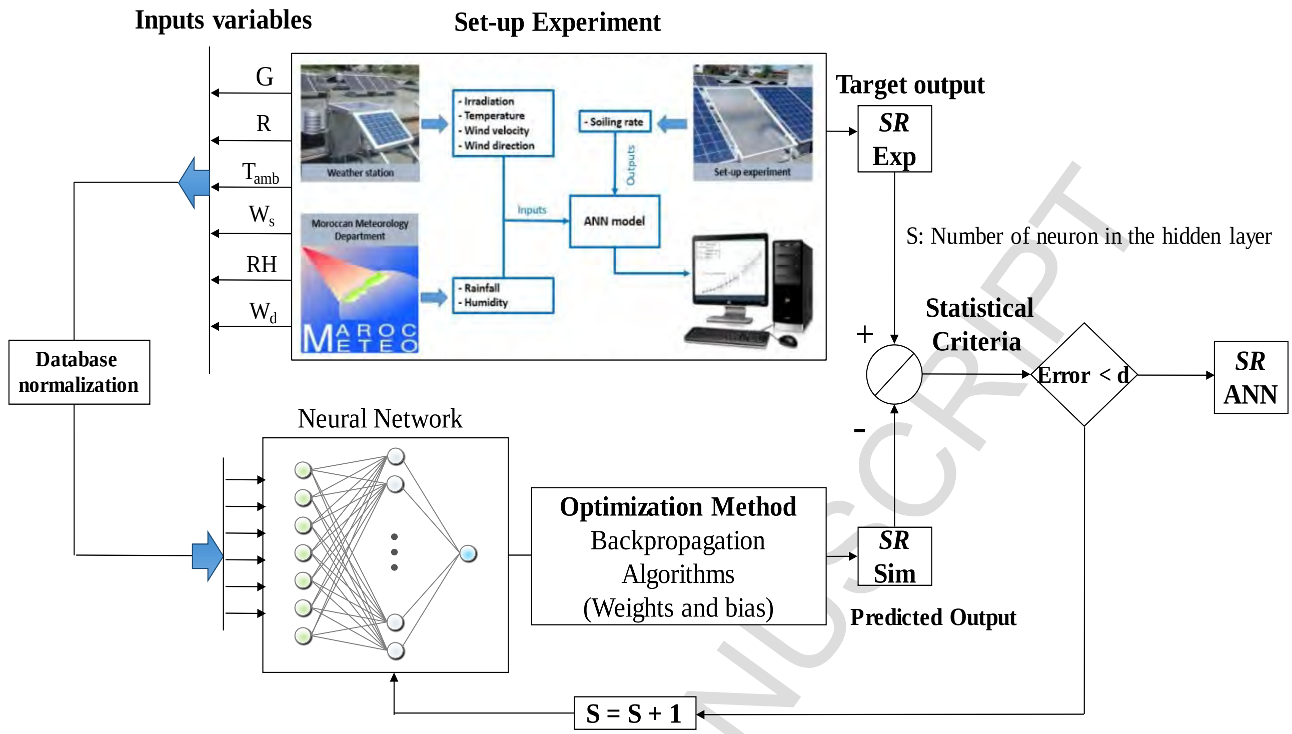

Figure 3. The numerical procedure used for the ANN learning process, and the iterative architecture used by the model to estimate soiling rate on PV modules.

2.4. *Global Sensitivity Analysis*

Global Sensitivity analysis (GSA) is a set mathematical techniques to understanding the relative contribution of the different input parameters ($x_i = x_1, x_2 \ldots x_M$) in the output response of a mathematical model (y). The use of GSA allows to identify the coherence of the model with the real world and determine if the relationship is adequate.

In the present work, PAWN sensitivity analysis was selected due its low computational cost and successful results in non-linear computational models [32]. This technique is based on calculating the sensitivity to input x_i as a measure of the distance between the unconditional cumulative distribution function of y ($F_y(y)$), obtained when all inputs vary simultaneously, and the conditional cumulative distribution functions ($F_{y|x_i}(y)$), obtained when varying all inputs with fixed x_i ($x_{\sim i}$). The Kolmogorov-Smirnov (KS) statistic is used to evaluate the distance between unconditional and conditionals cumulative distribution functions (CDFs):

$$KS = max_y \left| F_y(y) - F_{y|x_i}(y) \right| \quad (9)$$

As KS depends on the fixed value of x_i, it is calculated a PAWN sensitivity index (T_i) considering a statistic over all possible values of x_i:

$$T_i = \overset{stat}{\underset{x_i}{}} \left[KS(x_i) \right] \quad (10)$$

A numerical approximation is required to realize this procedure, illustrated in Figure 4. As it can be seen, it is divided in conditional and unconditional part. The unconditional CDF is approximated by evaluating N_u random samples, for all input parameters, in the mathematical model. On the other hand, to compute the conditionals CDF, g random samples are generated for each input parameter ($x_i = x_1, x_2 \ldots x_M$), called conditioning values. For each conditioning value, a conditional CDF is approximated using N_c output evaluations obtained keeping the g value for x_i fixed and sampling random the non-fixed inputs ($x_{\sim i}$). Finally, the KS statistic between unconditional and conditional CDFs is computed where KS distance indicates that the x_i parameter is very influential on the model output. The total number of model evaluations required to calculate the sensitivity value is $N_u + \mathrm{g} \times N_c \times M$. The values of g, N_c, and N_u are chosen by trial-and-error.

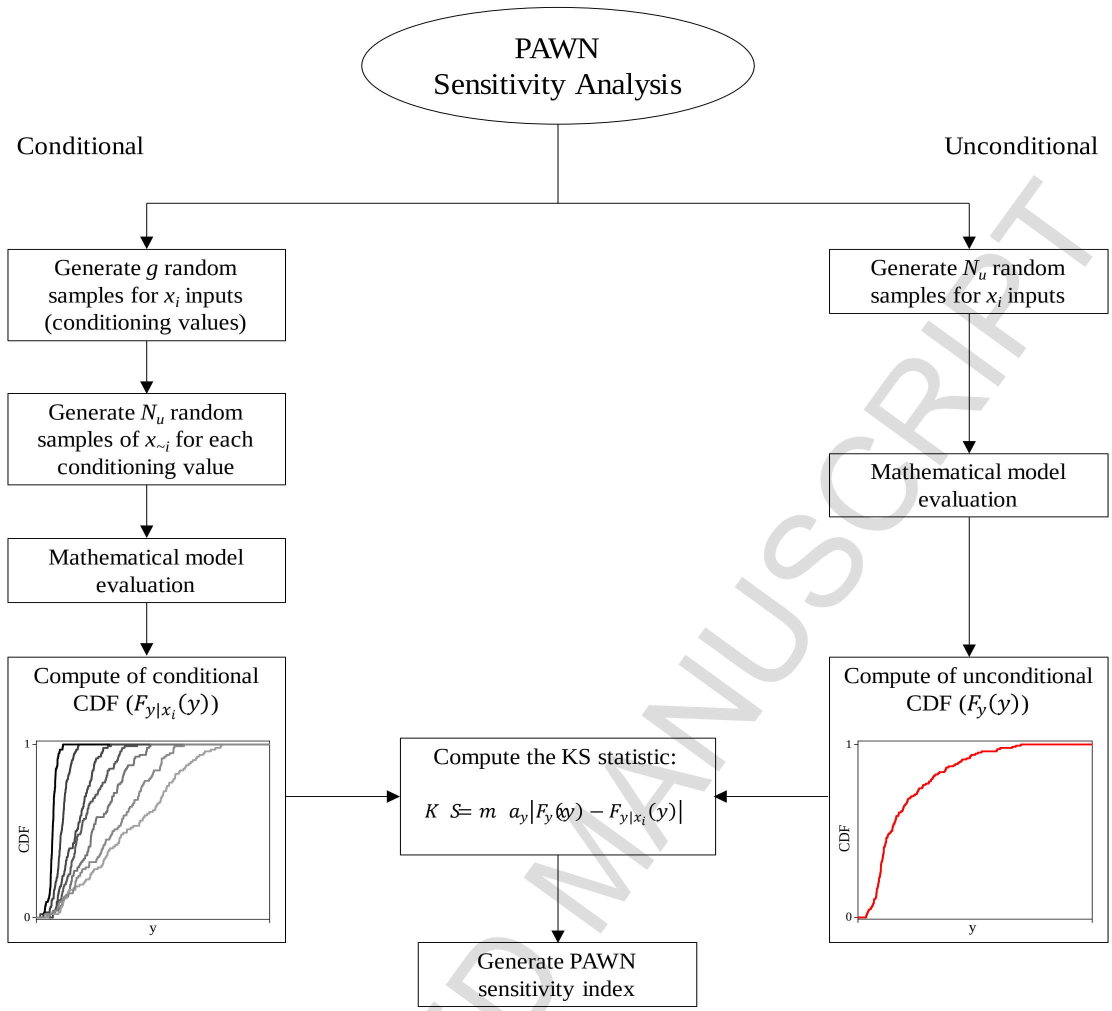

Figure 4. Schematic diagram of computational PAWN sensitivity analysis procedure.

3. RESULTS AND DISCUSSIONS

3.1. ANN model

In order to determine the optimal ANN architecture, several network configurations were trained and statistically compared (Eq. 6-8) varying the number of neurons in the hidden layer from 1-35. Mathematical software MATLAB and its ANN toolbox [28] were used to carry out the training process. Table 4 offers the results of the comparison between the simulated data obtained from the ANN architectures and experimental PV soiling rate measurements. According to Table 4, it can be noticed that the best ANN model prediction was obtained with 35 neurons in the hidden layer, generating a 6-35-1 ANN architecture (Figure 2). This model presents the smallest MAPE = 9.04 % and RMSE = 0.454.

Table 4. Artificial Neural Network architecture training results

ANN architecture	**RMSE**	**MAPE**	**R^2**	**Best linear fitting**
6-05-1	2.7527	32.8278	0.4727	y = 0.4633x + 4.6382
6-10-1	2.2664	25.7170	0.6271	y = 0.6252x + 3.2394
6-15-1	1.8280	19.4327	0.7579	y = 0.7558x + 2.1105
6-20-1	1.5040	13.9452	0.8346	y = 0.8346x + 1.4298
6-25-1	1.2318	10.8434	0.9051	y = 0.8224x + 0.9045
6-30-1	0.7597	9.2258	0.9175	y = 0.9075x + 0.4000
6-35-1	*0.4540*	*9.0398*	*0.9286*	*y = 0.9258x + 0.0288*

Figure 5 illustrates the linear regression fit between the experimental data and the results of the best ANN model using all the data available (training, testing, and validation). As it can be appreciated, the comparison between experimental (SR_{Exp}) and simulated (SR_{Sim}) obtained a satisfactory determination with a linear behavior fitting of R^2=92.8%, given by linear regression model:

$$SR_{Sim} = 0.9258 \times SR_{Exp} + 0.0288 \tag{11}$$

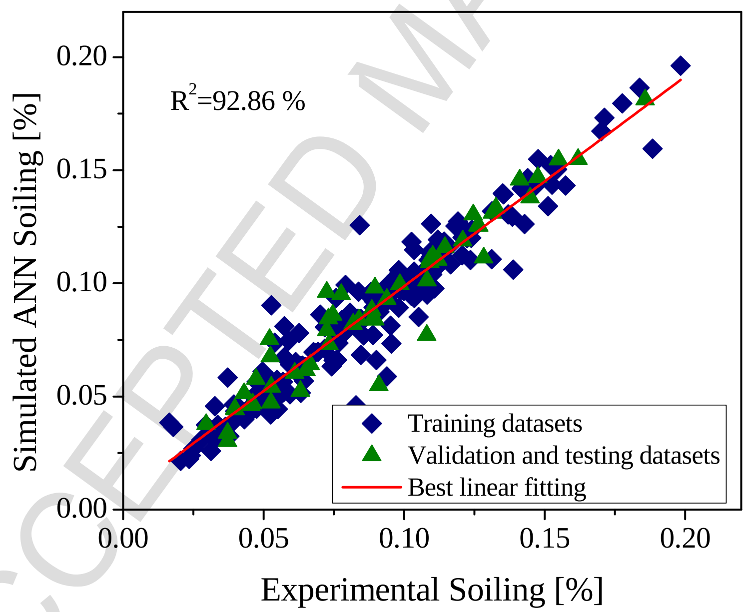

Figure 5. Statistical comparison between experimental soiling measurement and simulated soiling result from the best ANN architecture.

Table 5 enlists the optimum weights and bias obtained for the best ANN model, where IW and LW represent the input weights for the hidden layer and output layer respectively, K and S are the total input (K = 6) and neuron (S = 35) numbers, and b1 and b2 the bias factor.

Based on the developed ANN architecture (Figure 2), the logarithmic sigmoid transfer function (Eq. 4), the linear transfer function (Eq. 5), and the values presented in Table 5, the ANN model can be analytically represented by the following equation:

$$SR_{Sim} = \sum_{s=1}^{S}\left[LW(1,s)\left(\frac{1}{1+\exp\left(-2\left(\sum_{k=1}^{K}\left(IW(s,k)\,x(k)\right)+b_1(s)\right)\right)}\right)+1\right]+b_2 \quad (12)$$

where *x* is the parameter value corresponding operation and LW, IW, b1, b2, K, and S are described in Table 5.

Table 5. Weights and bias parameters obtained for the ANN model developed.

Hidden neurons (s)	**Weights**								
	Hidden layer (S=35, K=6) IW (s,k)						**Output layer LW(s,l)**	**Bias**	
	G (k=1)	**W_s (k=2)**	**W_d(k=3)**	**T_{amb}(k=4)**	**RH (k=5)**	**RF (k=6)**	**SR (%)**	**b1**	**b2**
1	-4.788	-0.289	-3.069	6.017	-1.715	-5.651	-14.478	-4.961	-1.930
2	1.800	-1.903	17.128	-1.227	-1.249	7.849	3.141	25.201	
3	-2.787	-0.861	-0.515	0.130	0.714	-3.057	14.848	-0.076	
4	-3.695	4.278	-0.741	2.866	5.506	4.479	-13.730	3.071	
5	-3.648	4.898	10.007	21.894	1.109	-5.269	-1.752	2.916	
6	0.913	2.801	6.207	0.125	-0.744	3.384	19.992	13.383	
7	5.879	3.290	7.435	7.199	3.376	3.441	7.910	0.820	
8	3.059	-5.496	2.105	-5.729	-2.937	15.189	-1.431	13.340	
9	4.908	0.545	4.856	-6.214	1.994	5.417	-12.475	6.272	
10	10.413	19.911	-6.890	-2.676	16.361	-7.085	0.693	-8.692	
11	-3.281	4.025	-0.186	2.688	4.820	4.645	15.518	3.960	
12	-13.070	-4.373	17.345	-15.929	-5.364	-5.184	-1.756	1.421	
13	5.920	-0.007	-8.455	-5.127	-6.689	6.924	6.312	-8.187	
14	-22.619	-4.441	8.296	13.944	-0.190	0.835	-0.468	11.735	
15	-2.749	-4.286	-2.032	-1.285	-1.173	0.002	-10.818	-0.686	
16	-9.973	-4.816	1.721	-44.492	-3.166	-2.532	0.571	11.219	
17	-11.632	-26.119	48.205	-23.840	-27.839	-4.195	-0.730	26.050	
18	6.304	-6.812	-10.102	6.815	-5.481	17.343	6.252	-4.118	
19	5.782	-2.033	6.166	-0.691	-1.799	12.291	5.382	6.947	
20	-37.417	12.972	-8.495	15.609	13.660	-16.278	-0.290	3.964	
21	-0.963	2.922	4.249	12.460	2.079	-5.783	3.087	-3.579	
22	-31.520	-17.327	-5.951	13.010	-7.637	-6.037	0.549	-6.039	
23	3.463	3.029	-5.686	0.088	3.747	6.629	1.679	7.869	
24	-12.464	-1.498	-3.459	-0.294	-4.565	2.364	4.955	-3.106	
25	-2.126	3.502	5.986	-3.452	2.703	-6.267	8.269	5.119	
26	-0.002	1.239	11.584	1.478	2.468	4.344	-2.512	14.643	
27	-9.983	2.081	-18.152	-4.788	6.500	-7.357	-1.035	-19.017	

28	-2.889	-3.748	-2.116	-1.278	-1.692	0.155	15.920	-0.064	
29	7.806	7.447	-0.222	-5.315	2.029	21.265	3.664	22.659	
30	2.205	2.057	0.332	0.313	2.199	-0.063	7.532	-1.882	
31	-0.494	-2.504	2.061	-0.282	-0.288	0.027	5.037	0.464	
32	5.828	-0.531	-15.515	-7.052	0.701	8.594	-1.983	-10.011	
33	-9.450	-7.380	-0.533	6.303	-1.810	-23.295	3.149	-25.229	
34	17.699	2.093	8.771	-1.912	2.641	-6.171	3.342	7.265	
35	2.413	5.784	-0.052	10.588	1.246	2.347	-16.369	16.283	

3.2. Sensitivity analysis results

Sensitivity analysis was carried out using the computational package SAFE 1.1 [33]. The assigned N_u, N_c, and g values were 1200, 900, and 45 respectively, obtained by an iterative evaluation procedure. The N_u and N_c random samples were generated considering the minimum and maximum values of each parameter (Table 3). Figure 6 illustrates the unconditional and conditional CDFs output response of the PV glass soiling rate model developed. The red lines represent the unconditional CDFs ($F_y(y)$), and the gray-scale lines are the conditional CDFs ($F_{y|x_i}(y)$) at different fixed values of the analyzed parameter (x_i).

As it can be seen in Figure 6, the $F_{y|x_i}(y)$ curves of input parameters present different cumulative densities distanced of their respective $F_y(y)$. This behavior indicates the effect of x_i on the PV glass soiling rate predicted. In the case of relative humidity, wind direction, and wind speed, a greater separation distance between $F_{y|x_i}(y)$ and $F_y(y)$ curves are observed. This indicates that these parameters have a significant effect on the model response. On the contrary, for rainfall and ambient temperature, the curves $F_{y|x_i}(y)$ approximate to $F_y(y)$ determining that both parameters have less influence on the model output.

Figure 6 also provides information about the model behavior when modifying the value of the fixed input parameter from lowest (dark $F_{y|x_i}(y)$ lines) to greater (clear $F_{y|x_i}(y)$ lines). It can be observed in Figure 6(a), that increments in the solar irradiance values decrease the model output response, while higher dust deposition occurs in the presence of low radiation. Similar case is presented in Figure 6(b), where according to the model the soiling deposition is favored by the low wind velocities, which is consistent with the physical behavior of the phenomenon. On the other hand, from Figure 6(c) and 6(e), it is observed that the soling rate is directly proportional to variations of wind direction and relative humidity. Finally, for ambient temperature and rainfall (Figure 6(d) and 6(f)) it is not possible to make a clear description due to the low sensitivity they present.

A sensitivity index (T_i) is calculated considering a statistic over all possible values of x_i in order to synthesize the cumulative density distribution curves analysis results. The T_i provides a value that describes the model sensitivity respect to the variable. Table 6 shows the summarizes sensitivity analysis information. T_i results indicate that relative humidity was the most significant parameter (0.2122) for PV soiling deposition following by wind direction (0.2103), wind speed (0.1778), solar radiation (0.1733), ambient temperature (0.1689), and rainfall (0.1458). It is important to indicate that the indexes of the parameters are close to each other. It determines that although the influence of some is smaller their contribution is important for the modeling process.

Table 6. Relative importance of input variables.

Parameter	**Sensitivity Index**
Solar irradiance	0.1733
Wind speed	0.1778
Wind direction	0.2103
Ambient temperature	0.1689
Relative humidity	0.2122
Rainfall	0.1458

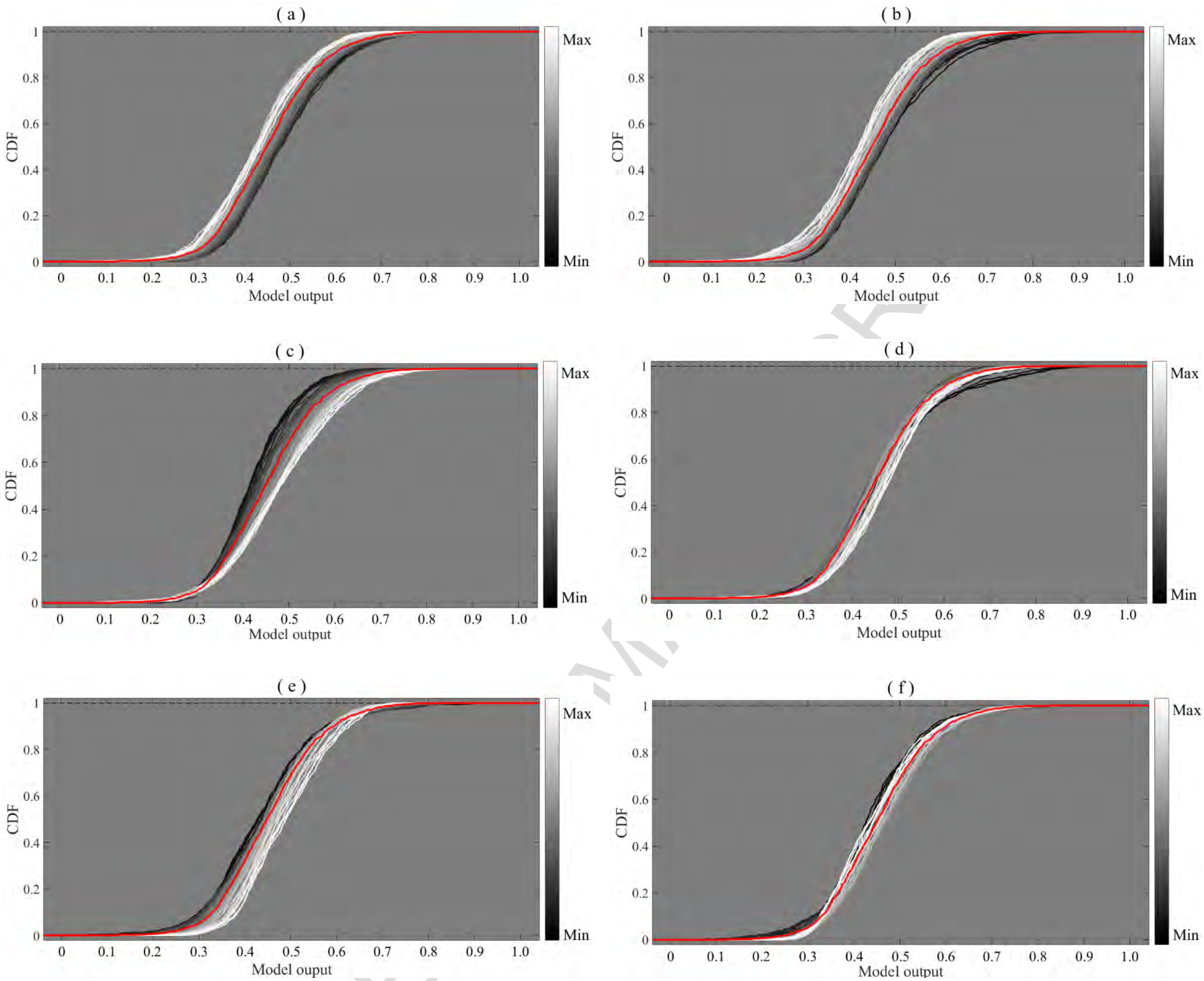

Figure 6. Cumulative density distribution curves of the model output for each input parameters. (a) solar irradiance, (b) wind speed, (c) wind direction, (d) ambient temperature, (e) relative humidity, (f) rainfall.

4. CONCLUSIONS

This paper proposed a computational methodology for estimation of soiling rate on solar PV panels. An Artificial Neural Network (ANN) model was developed to express the soiling rate in function of the environmental parameters solar irradiance, wind speed, wind direction, ambient temperature, relative humidity, and rainfall. The model was trained with experimental data from Moroccan Meteorology Department and Solar Energy Platform in Rabat, Morocco. The performance of the model was statistically evaluated and compared with information not used in the modeling process. The statistical results indicate that the ANN model has an adequate estimation capacity for the given conditions of the case study.

In addition, a new sensitivity analysis technique is employed to determine the effects of input parameters in the response of the ANN model. The sensitivity analysis results indicate that all the parameters have a relevant contribution on model output, begging the most influential the relative humidity followed by wind direction, wind speed, solar irradiance, ambient temperature, and rainfall. Sensitivity analysis also showed the behavior of the model output for variation of each input parameter in a wide range value (from maximum to minimum). This provides a more detailed description of the model allowing to visualize its ability to adapt to the phenomenon of study.

This work lays the foundation for modeling based on more detailed artificial intelligence techniques that consider greater geographic extensions, different annual conditions and longer periods of measurement. On the other hand, it was also demonstrated that the employed sensitivity analysis proves to be a powerful tool that allows describing the physics of the phenomenon from the ANN model.

This kind of analysis can be implemented in other renewable energy model based on artificial intelligence to complete the empty knowledge that leaves the use of these techniques in the physical understanding of the phenomenon. Finally, this method is a promising framework for its application in smart sensors on cleaning systems for PV modules to improve their operational efficiency.

ACKNOWLEDGES

This work was developed in the framework of SOLEIL Inno-PV project, co-financed by the Moroccan Research Institute IRESEN (Institut de Recherche en Energie Solaire et Energies Nouvelles), and as part of CONACYT-SENER 254667 project.

The authors are thanking Prof. Moulay Abdelmjid Sebbar, Mis. Fadwa Safsafi, and Mis. Fatima-ez-zahrae Daoudi from PSES Research Team, for their valuable scientific and technical contributions.

REFERENCES

[1] OECD, Public-Private Partnerships in the Middle East and North Africa. A Handbook for Policy Makers, (2014) 121.

[2] S. Bouaddi, A. Ihlal, A. Fernández-García, Soiled CSP solar reflectors modeling using dynamic linear models, Sol. Energy. 122 (2015) 847–863. doi:10.1016/j.solener.2015.09.044.

[3] M. Karim, S. Naamane, C. Delord, Evaluation of the behaviour of different solar mirrors against soiling phenomenon, in: 2016 Int. Renew. Sustain. Energy Conf., IEEE, 2016: pp. 326–329. doi:10.1109/IRSEC.2016.7984008.

[4] A.A. Merrouni, F. Wolfertstetter, A. Mezrhab, S. Wilbert, R. Pitz-Paal, Investigation of Soiling Effect on Different Solar Mirror Materials under Moroccan Climate, Energy Procedia. 69 (2015) 1948–1957. doi:10.1016/j.egypro.2015.03.194.

[5] C. Schill, S. Brachmann, M. Koehl, Impact of soiling on IV-curves and efficiency of PV-modules, Sol. Energy. 112 (2015). doi:10.1016/j.solener.2014.12.003.

[6] P. Sinha, W. Hayes, B. Littmann, L. Ngan, R. Znaidi, Environmental variables affecting solar photovoltaic energy generation in Morocco, in: 2014 Int. Renew. Sustain. Energy Conf., IEEE, 2014: pp. 230–234. doi:10.1109/IRSEC.2014.7059897.

[7] W. Anana, F. Chaouki, B. Laarabi, D. Dahlioui, M.A. Sebbar, A. Barhdadi, V. Gilioli, D. Verdilio, Soiling impact on energy generation of high concentration Photovoltaic power plant in Morocco, in: 2016 Int. Renew. Sustain. Energy Conf., IEEE, 2016: pp. 234–238. doi:10.1109/IRSEC.2016.7983994.

[8] D. Dahlioui, B. Laarabi, M.A. Sebbar, A. Barhdadi, G. Dambrine, E. Menard, J. Boardman, Soiling effect on photovoltaic modules performance: New experimental results, in: 2016 Int. Renew. Sustain. Energy Conf., IEEE, 2016: pp. 111–114. doi:10.1109/IRSEC.2016.7983955.

[9] S. Bouaddi, A. Ihlal, A. Fernández-García, Comparative analysis of soiling of CSP mirror materials in arid zones, Renew. Energy. 101 (2017) 437–449. doi:10.1016/j.renene.2016.08.067.

[10] D.C. Miller, S.R. Kurtz, Durability of Fresnel lenses: A review specific to the concentrating photovoltaic application, Sol. Energy Mater. Sol. Cells. 95 (2011) 2037–2068. doi:10.1016/j.solmat.2011.01.031.

[11] T. Sarver, A. Al-Qaraghuli, L.L. Kazmerski, A comprehensive review of the impact of dust on the use

of solar energy: History, investigations, results, literature, and mitigation approaches, Renew. Sustain. Energy Rev. 22 (2013) 698–733. doi:10.1016/j.rser.2012.12.065.

[12] H.K. Elminir, A.E. Ghitas, R.H. Hamid, F. El-Hussainy, M.M. Beheary, K.M. Abdel-Moneim, Effect of dust on the transparent cover of solar collectors, Energy Convers. Manag. 47 (2006) 3192–3203. doi:10.1016/j.enconman.2006.02.014.

[13] M.S. El-Shobokshy, F.M. Hussein, Effect of dust with different physical properties on the performance of photovoltaic cells, Sol. Energy. 51 (1993) 505–511. doi:10.1016/0038-092X(93)90135-B.

[14] H. Khonkar, A. Alyahya, M. Aljuwaied, M. Halawani, A. Al Saferan, F. Al-khaldi, F. Alhadlaq, B.A. Wacaser, Importance of cleaning concentrated photovoltaic arrays in a desert environment, Sol. Energy. 110 (2014) 268–275. doi:10.1016/j.solener.2014.08.001.

[15] J. Yun, L. Verma, A. James, H. Yang, The Effect of Dust on Transmission and Self-cleaning Property of Solar Panels, 15 (2012) 421–427. doi:10.1016/j.egypro.2012.02.051.

[16] A. Sayyah, M.N. Horenstein, M.K. Mazumder, Energy yield loss caused by dust deposition on photovoltaic panels, Sol. Energy. 107 (2014) 576–604. doi:10.1016/j.solener.2014.05.030.

[17] R. De Leone, M. Pietrini, A. Giovannelli, Photovoltaic energy production forecast using support vector regression, Neural Comput. Appl. 26 (2015) 1955–1962. doi:10.1007/s00521-015-1842-y.

[18] R.V.A. Monteiro, G.C. Guimarães, F.A.M. Moura, M.R.M.C. Albertini, M.K. Albertini, Estimating photovoltaic power generation: Performance analysis of artificial neural networks, Support Vector Machine and Kalman filter, Electr. Power Syst. Res. 143 (2016) 643–656. doi:10.1016/j.epsr.2016.10.050.

[19] J. Tziu Dzib, E.J. Alejos Moo, A. Bassam, M. Flota-Bañuelos, M.A. Escalante Soberanis, L.J. Ricalde, M.J. López-Sánchez, Photovoltaic Module Temperature Estimation: A Comparison Between Artificial Neural Networks and Adaptive Neuro Fuzzy Inference Systems Models, in: Intell. Comput. Syst., 2016: pp. 46–60. doi:10.1007/978-3-319-30447-2.

[20] A. Bassam, O. May Tzuc, M.A. Escalante Soberanis, L.J. Ricalde, B. Cruz, Temperature Estimation for Photovoltaic Array Using an Adaptive Neuro Fuzzy Inference System, Sustainability. 9 (2017) 1399. doi:10.3390/su9081399.

[21] A.A.A. Darwish, T.A. Hanafy, A.A. Attia, D.M. Habashy, M.Y. El-Bakry, M.M. El-Nahass, Optoelectronic performance and artificial neural networks (ANNs) modeling of n-InSe/p-Si solar cell, Superlattices Microstruct. 83 (2015) 299–309. doi:10.1016/j.spmi.2015.03.033.

[22] M. Kamran, S.A. Haider, T. Akram, S.R. Naqvi, S.K. He, Prediction of IV curves for a superconducting thin film using artificial neural networks, Superlattices Microstruct. 95 (2016) 88–94. doi:10.1016/j.spmi.2016.04.018.

[23] R.K. Kharb, S.L. Shimi, S. Chatterji, M.F. Ansari, Modeling of solar PV module and maximum power point tracking using ANFIS, Renew. Sustain. Energy Rev. 33 (2014) 602–612. doi:10.1016/j.rser.2014.02.014.

[24] S. Haykin, Neural networks, Upper Saddle River, NJ Prentice Hall., 1999.

[25] A. Espinosa Guzmán, O. May Tzuc, I. Balam Pantí, J. Reyes Trujeque, I. Pérez Quintana, A. Bassam,

Modelado de partículas PM10 y PM2.5 Mediante Redes Neuronales Artificiales sobre clima tropical de San Francisco de Campeche, México, Quim. Nova. In Press (2017) 1–10. doi:10.21577/0100-4042.20170115.

[26] A.M. Ghaedi, M. Ghaedi, A.R. Pouranfard, A. Ansari, Z. Avazzadeh, A. Vafaei, I. Tyagi, S. Agarwal, V.K. Gupta, Adsorption of Triamterene on multi-walled and single-walled carbon nanotubes: Artificial neural network modeling and genetic algorithm optimization, J. Mol. Liq. 216 (2016) 654–665. doi:10.1016/j.molliq.2016.01.068.

[27] O. May Tzuc, A. Bassam, M.A. Escalante Soberanis, E. Venegas-Reyes, O.A. Jaramillo, L.J. Ricalde, E.E. Ordoñez, Y. El Hamzaoui, Modeling and optimization of a solar parabolic trough concentrator system using inverse artificial neural network, J. Renew. Sustain. Energy. 9 (2017) 13701. doi:10.1063/1.4974778.

[28] M.H. Beale, M.T. Hagan, H.B. Demuth, Neural Network Toolbox™ User's Guide R2017a, The MathWorks, Inc., 2017.

[29] J. de Villiers, E. Barnard, Backpropagation Neural Nets with One and Two Hidden Layers, IEEE Trans. Neural Networks. 4 (1993) 136–141. doi:10.1109/72.182704.

[30] S.K. Biswas, M. Chakraborty, H.R. Singh, D. Devi, B. Purkayastha, A.K. Das, Hybrid case-based reasoning system by cost-sensitive neural network for classification, Soft Comput. (2016) 1–18. doi:10.1007/s00500-016-2312-x.

[31] Y. El Hamzaoui, M. Abatal, A. Bassam, F. Anguebes-Franseschi, O. Oubram, I. Castaneda Robles, O. May Tzuc, Artificial neural networks for modeling and optimization of phenol and nitrophenols adsorption onto natural activated carbon, Desalin. Water Treat. 58 (2017) 2002–213. doi:10.5004/dwt.2017.1705.

[32] F. Pianosi, T. Wagener, A simple and efficient method for global sensitivity analysis based on cumulative distribution functions, Environ. Model. Softw. 67 (2015) 1–11. doi:10.1016/j.envsoft.2015.01.004.

[33] F. Pianosi, F. Sarrazin, T. Wagener, A Matlab toolbox for Global Sensitivity Analysis, Environ. Model. Softw. 70 (2015) 80–85. doi:10.1016/j.envsoft.2015.04.009.

Highlights

- An artificial neural network methodology has been proposed for modeling soiling rate on solar photovoltaic glass.
- Artificial neural network was trained and testing using environmental variables.
- Statistical criteria were employed to measure the error between experimental and the predicted results.
- A sensitivity analysis approach was employed to determine the effect of input parameter on model output.